Chinese Journal of Chemical Engineering 51 (2022) 75–85

Contents lists available at ScienceDirect

Chinese Journal of Chemical Engineering

journal homepage: www.elsevier.com/locate/CJChE

Full Length Article

Fe_3O_4-carbon spheres core–shell supported palladium nanoparticles: A robust and recyclable catalyst for suzuki coupling reaction

Mohamed A. Almaradhi, Hassan M.A. Hassan, Mosaed S. Alhumaimess *

Department of Chemistry, College of Science, Jouf University, PO Box 2014, Sakaka, Saudi Arabia

ARTICLE INFO

Article history:
Received 7 August 2021
Received in revised form 2 October 2021
Accepted 15 November 2021
Available online 04 January 2022

Keywords:
Heterogeneous catalysis
Aryl halide
Suzuki coupling
Palladium nanoparticles
Carbon spheres

ABSTRACT

Suzuki-Miyaura (S-M) is regarded the most powerful way for synthesis biaryls, triaryls, or incorporating of substituted aryl moieties in organic preparation by the cross-coupling of aryl boronic acid with aryl halides using the Pd catalyst. This work reports the combining of the hydrothermal and microwave-assisted protocol to convert the glucose to magnetic carbon spheres (Fe_3O_4-CSPs) decorated with Pd nanoparticles (NPs) as the catalyst for Suzuki-Miyaura cross-coupling reactions. The physicochemical properties in the produced composite were examined using FESEM, HRTEM, nitrogen isotherms, Raman spectroscopy, FTIR, XPS, and XRD. The as-fabricated composite Pd/Fe_3O_4-CSPs is mostly spherical with a core–shell structure and possesses a great surface area of 253.2 $m^2 \cdot g^{-1}$. Its catalytic performance demonstrates that the composite has excellent stability and high tolerance Suzuki-Miyaura cross-coupling reactions in 30 min at 80 °C. Both activated and deactivated aryl halides provided excellent yield. The as-fabricated catalyst was recycled for up to four catalytic cycles without a substantial decline in performance. Moreover, this research offers a facile roadmap for synthesizing Pd/Fe_3O_4-CSPs composites and promoting the practical implementation of Pd/Fe_3O_4-CSPs catalysts for organic transformation processes.

1. Introduction

Due to their numerous advantages in industrialized uses, heterogeneous catalysis systems have gained great interest in recent decades, such as feasible separation from the chemical process and substantial durability [1,2]. Researchers have concentrated mainly on nanoscale composites among the different heterogeneous catalysis models due to their enormous active surface area and exceptional functionalization performance [3,4]. Carbon-based composites are one well-known nonmetric catalytic material, particularly in the last few decades. Carbon is plentiful on earth as a non-mental component and plays a major role in various applications. Carbon materials predominantly comprise carbon atoms in which microstructures and morphologies exhibit enormous variety. Carbon materials have a wide collection of carbon comprising mesoporous carbon, graphene, carbon sphere, carbon nanotube, carbon fiber, and quantum dots [5–14]. Within this large carbon family, carbon spheres are of major relevance as carbon-based materials possess great surface areas and common geometries. Various fabrication parameters can tune the pores size distribution and porosity shape *via* appropriate development approaches [15]. Carbon spheres were commonly applied in a variety of applications, including removal [16,17], supports [18], batteries [19], and supercapacitors [20,21]. Cross-coupling transformations have usually been carried out under homogeneous procedures [22–26]. However, owing to the scarcity of durability and possible pollution from remaining metals in the development product, the problems connected with homogeneous catalysis continue to concern for various applications of these catalytic methods [27,28]. Major endeavors have been undertaken to promote the production of C—C coupling catalysts in which the metallic palladium nanoparticles are immobilized on supports like nanomaterials [29–33], activated carbon [34], or zeolites [35,36] to tackle this problem. A decrease in the performance of the immobilized metallic nanoparticle is commonly noted, although heterogeneous supports enable powerful recycling. The tailoring of heterogeneous metallic palladium catalysts that comprise high performance, stability, and reusability is an essential objective of research into nanomaterials that is likely to have a major future effect on various industries. Suzuki-Miyaura (S-M) is considered the most powerful approach for preparing biaryls, triaryls, or incorporating of

* Corresponding author.
E-mail address: mosaed@ju.edu.sa (M.S. Alhumaimess).

https://doi.org/10.1016/j.cjche.2021.11.024

substituted aryl groups in organic preparation by the cross-coupling of aryl boronic acid with aryl halides using the Pd catalyst. While several Pd catalysts for the S-M reaction were used [37–39], a quick and potential heterogeneous catalysis by this Pd-carbon sphere (CSPs) was not recorded to a large extent. Besides, CSP-based nanocatalysts might well be expected to display great catalytic performance because of the large surface areas, common geometries, and less complicated fabrication approach using eco-friendly chemicals of CSPs compared to other support materials. Thus, it is desirable to explore an effective strategy for developing magnetically recoverable and incredibly effective palladium supported CSPs Suzuki-Miyaura catalyst.

Herein, we report a hydrothermal approach for the fabrication of magnetically recoverable Fe_3O_4-CSPs composites. The carbon spheres (CSPs) were made using a hydrothermal process of glucose as a carbon precursor and carbonization at 700 °C. Without chemical additives, the fabrication process is green, simple, eco-friendly, and template-free. The Fe_3O_4-CSPs support were used to immobilize Pd nanoparticles results in a significant improvement of the activity of the Pd nanoparticles in the solid Pd/Fe_3O_4-CSPs catalyst for the Suzuki coupling reactions with unparalleled catalytic performance approaching that of the current homogeneous Pd catalysts.

2. Experimental

2.1. Chemicals

All presented materials were provided as obtained without any further purification. phenylboronic acid (95%), 1-bromobenzene (≥99%), 4-bromoacetophenone (98%), 3-bromoacetophenone (98%), 2-bromoacetophenone (98%), 4-bromobenzonitrile (98%), 1-bromo-4-nitrobenzene (98%), 2-bromoanisole (98%), 4-bromotoluene (98%), palladium (II) nitrate (99.99%), Sodium acetate (CH_3COONa, ≥ 99%), dichloromethane anhydrous (≥99.8%), chloroform (≥99.5%), potassium carbonate (K_2CO_3, ≥ 99.9%) were procured from Sigma-Aldrich Co., USA. Acros Organics supplied ethanol (99.5%). D (+) Glucose used to prepare CSPs was obtained from Merck KGaA Co., Germany. Sodium sulphate (99+%) and $FeCl_3{\cdot}6H_2O$ (99+%) were provided from Fisher Scientific Co., UK. Distilled water provided in all measurements was obtained by Milli-Q direct 8 purification system (Millipore, France).

2.2. Materials

2.2.1. Preparation of carbon spheres (CSPs)

Typically, by the aid of sonication, 5.0 g of D(+) glucose anhydrous was soluble in 50 ml of DI water, then added the glucose solution to a 75 ml Teflon-lined stainless steel autoclave. The autoclave was tightly closed and slowly heated to 180 °C in a furnace for 10 h. The intense brown products obtained were gathered by simple filtration, washed with deionized water and ethanol many times, and dried overnight at 80 °C. Finally, the CSPs were obtained by calcinating of the polymerized glucose at 700 °C for 4 h with a heating rate of 5 (°)·min^{-1} under the flow of nitrogen gas in a programmable tube furnace [40,41] (Fig. 1).

2.2.2. Synthesis of magnetically carbon spheres Fe_3O_4-CSPs

The CSPs (0.5 g) were typically sonicated for 2 h in ethylene glycol (30 ml). A mixture of (0.9375 g) $FeCl_3{\cdot}6H_2O$ and (2.4 g) sodium acetate was introduced to the dispersed CSPs with continuous sonicating at 50 °C for 1 h to form a homogeneous blend. Then, the dispersed mixture was moved to a 50 ml Teflon-lined stainless steel autoclave. The autoclave was tightly closed and heated in a furnace for 10 h at 200 °C and then kept cooling down to ambient temperature. Finally, with the assist of a magnet, the product (Fe_3O_4-CSPs) were magnetically isolated, and rinsed several cycles with DI water and ethanol and dried at 80 °C for 12 h (Fig. 1).

2.2.3. Synthesis of Pd@ Fe_3O_4-CSPs composite

In deionized water (30 ml), the Fe_3O_4-CSPs (0.5 g) were first sonicated for 1 h until uniform suspension was achieved. A calculated amount of palladium nitrate was then introduced with continuous sonicating for a further 1 h. After adding 50 µl of the hydrazine hydrate, the solution was put inside a domestic microwave. For a total reaction time of 120 s, the microwave oven was then worked at maximum output in 40 s cycles (on for 20 s, off and stirring for 20 s). Finally, with the aid of a magnet, the Pd/Fe_3O_4-CSPs catalyst were magnetically separated and dried overnight under a vacuum (Fig. 1).

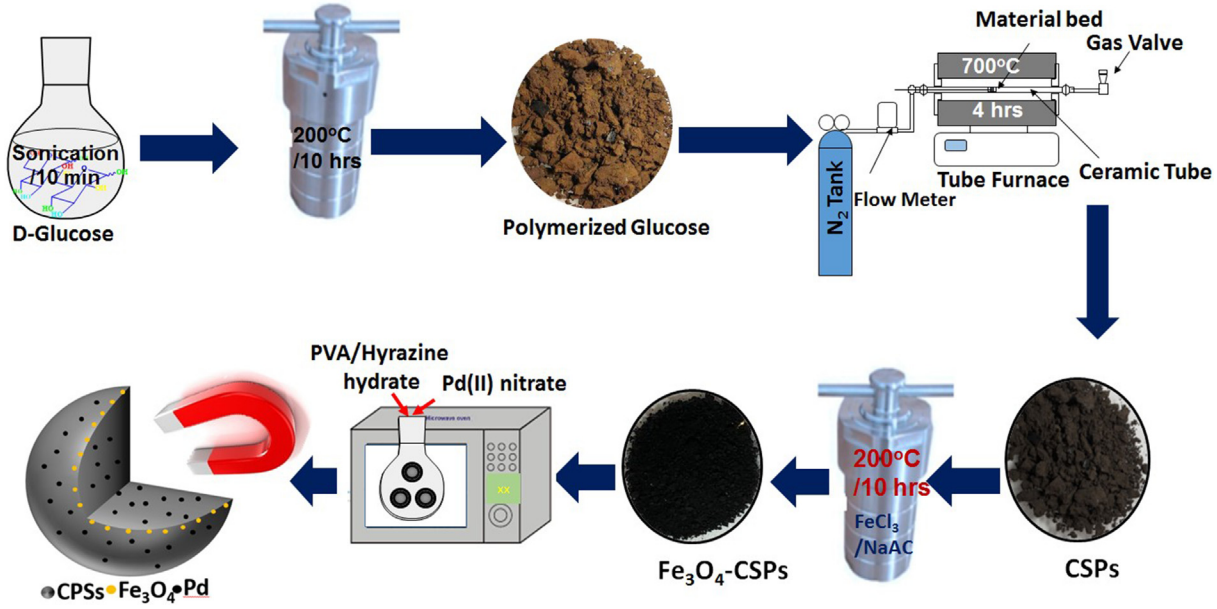

Fig. 1. Schematic representation emphasizing the preparation of Pd/Fe_3O_4-CSPs catalyst.

2.3. Characterization

X-ray diffraction (XRD) was conducted X-ray di_ractometer Maxima–X (D/Max2500VB2+/Pc, Shimadzu, Kyoto, Japan) diffractometer at 40 kV and 40 mA with Cu-K_α radiation. FTIR spectra were collected in the 4000–400 cm^{-1} range by Shimadzu IR Tracer-100 (Shimadzu, Kyoto, Japan). X-ray photoelectron spectroscopy (XPS) measurements on K-ALPHA (Thermo Fisher Scientific, Dreieich, Germany) was operated. The N_2 isotherms and surface characteristics were obtained at 77 K using A NOVA 4200e (Quantachrome Instruments, Quantachrome, Boynton Beach, USA). Thermogravimetric profiles (TGA) were conducted on TGA-51 Shimadzu (25–600 °C, 10 °C·min^{-1}, under flowing air gas). The morphological structure of the catalyst were investigated by the field emission scanning electron microscopy (FESEM, Thermo Scientific Quattro ESEM, Thermo Fisher, Waltham, MA, USA). High-resolution transmission electron microscopy (HRTEM) images were obtained using a JEOL2011 electron microscope operated at 200 kV. The Suzuki coupling reaction product was monitored by NMR-Jeol 600.

2.4. Catalytic performance

In a magnetically stirred round, bottom flask at 30 °C in ethanol, the Suzuki-Miyaura reaction of phenylboronic acid and an aryl halide utilizing Pd/Fe_3O_4-CSPs as the catalyst in the existence of K_2CO_3 as a basic material was performed. A blend of phenylboronic acid (135 mg, 1.1 mmol) and 4-bromoacetophenone (200 mg, 1.0 mmol) was soluble in 15 ml of ethanol in a 50 ml round-bottom flask and 5 mg Pd/Fe_3O_4-CSPs and (138 mg, 1 mmol) of K_2CO_3 was introduced to the reaction mixture. After that, the blend was agitated for 30 min at 80 °C. Upon completion of the reaction time, a magnet was utilized to separate the Pd/Fe_3O_4-CSPs catalyst from the reaction mixture. Dichloromethane/chloroform treated with Na_2SO_4 was used to extract biphenyl and unreacted aryl halides (if detected). After filtration, the dichloromethane was separated using rotary evaporation under reduced pressure. The products were dissolved in $CDCl_3$, and ^1H NMR was applied to analyse them. The yield was estimated by comparing the signals integration values of both biphenyl with the unreacted aryl halide. The yield (%) was estimated for the reaction between bromobenzene and $PhB(OH)_2$, by compared the integral of the signal at δ 7.41 (biphenyl) with those at δ 7.2 (unreacted bromobenzene). The yield assign to various aryl halide conversion was also based on ^1H NMR (Section S1, Fig. S1-1 – S1-7 in the Supplementary Material).

2.5. Catalyst recyclability

To emphasize the durability of Pd/Fe_3O_4-CSPs in the Suzuki-Miyaura, the recyclability tests were performed by selecting the reaction between phenylboronic acid with 4-bromoacetophenone as a model reaction. The catalyst was also isolated by a magnet's aid after each reaction and washed thoroughly with methanol–water (8:2) blend under continuous stirring (~3 times, each time for ~30 min). The separated catalyst was dried overnight at 120 °C and used for the next experiment.

2.6. Leaching performance experiment

The Pd/Fe_3O_4-CSPs were retrieved from the reaction vessel at 80 °C after 10 min. The filtrate was split into two parts: the first part was further operated for 30 min at 80 °C and, NMR tracked the other.

3. Results and Discussion

3.1. Spectroscopic characterization

FT-IR spectra are employed to confirm the hydrothermal synthesis of the carbon spheres composite. Fig. 2(a) showed the spectra of the glucose precursor, polymerized glucose (as grown), Fe_3O_4-CSPs, and Pd/Fe_3O_4-CSPs composite. The spectrum of the polymerized glucose (as grown CSPs) comprising the following bands: wide absorption band from 3000–3500 cm^{-1} is ascribed to OH stretching, weak band at 2900 cm^{-1} related to stretching modes of C—H aliphatic, absorption peaks at 1614 and 1709 cm^{-1} are respectively ascribed to C=C, and C=O modes, the characteristics absorption bands in the range of 1000–1500 cm^{-1} assigned to stretching C—OH and bending O—H modes, and peaks in between 500–900 cm^{-1} are essentially connected to bending C—H. The obtained results demonstrated the incidence of aromatization and polymerization (as grown CSPs) during the glucose hydrothermal process [40–43]. Once the polymerized glucose (as grown CSPs) was calcined at 700 °C, the bands at 2900, 1700, and, in the range of 1000–1500 cm^{-1} vanished, indicating further elimination of a huge number of oxygen-containing moieties

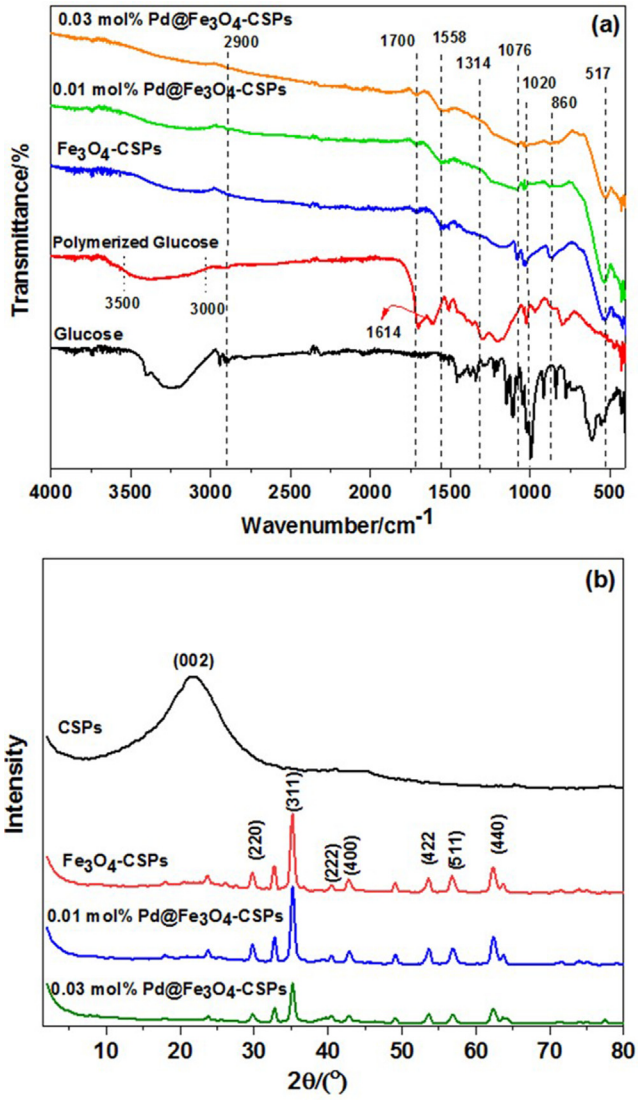

Fig. 2. (a) FT-IR spectra, and (b) XRD diffraction patterns of CSPs and Fe_3O_4-CSPs catalyst containing various dosage of Pd.

present on the CSPs surface. Furthermore, the absorption band at 517 cm^{-1}, ascribed to the Fe—O vibrations, confirming the coating of CSPs surface with magnetite. It should be noted that the FTIR spectra of Pd/Fe_3O_4-CSPs composite are nearly identical to that of the pristine Fe_3O_4-CSPs. However, the intensity of the absorption bands becomes relatively weaker, suggesting the surface functional groups of the Fe_3O_4-CSPs remained unchanged after the immobilization of Pd nanoparticles.

To emphasize and verify the successful synthesis of Fe_3O_4-CSPs magnetic composite, XRD was conducted. Two diffraction peaks persisted at 2θ value of 22° and 43.7° in the XRD patterns (Fig. 2 (b)) of the pristine CSPs, that were assigned to the crystal plane (0 0 2) and (1 0 0) of the graphite materials, respectively [14]. The consequence of low crystalline phase and a massive number of structural disorder is the broadening of peaks. Moreover, the decoration of CSPs with Fe_3O_4 resulted in five diffraction peaks at 29.7°, 35.04°, 42.6°, 56.8°, and 62.5°, related to (2 2 0), (3 1 1), (4 0 0), (5 1 1) and (4 4 0) of Fe_3O_4 (PDF#19-0629), respectively. Besides, the XRD pattern did not display distinctive diffraction peaks of Pd nanoparticles, suggesting that Pd nanoparticles were fruitful dispersion within the porous structure of the CSPs.

To further affirm the transformation of glucose to CSPs, Raman spectra are displayed in Fig. 3. The Raman spectrum of CSPs is displayed by two definite bands, the G band at 1595 cm^{-1}, and the D band at 1380 cm^{-1} [40]. The G band contributes to the E_{2g} mode of graphite mode ascribed to the two-dimensional hexagonal lattice vibration sp^2-carbon atoms. The D band, on the other hand, refers to the defects in the graphitic structure. The Raman spectrum of Pd/Fe_3O_4-CSPs composite displayed the same band at 1593 and 1390 cm^{-1} which also ascribed to G and D modes. Besides, a definite D/-shoulder at about 1616 cm^{-1} was also observed in Pd/Fe_3O_4-CSPs composite due to the disorders of the structure at the defect centers. It is worth noting that the intensity ratio (I_D/I_G) is calculated to determine carbon matrix quality since this ratio nearly zero for highly order carbon [44]. I_D/I_G value of the CSPs coating with Pd/Fe_3O_4, rises from 0.36 of pure CSPs to 0.70 of Pd/Fe_3O_4-CSPs, suggesting an increase of defects or disorders carbon matrix [44] that can lead to enhancement in the catalytic process.

3.2. Thermal stability

TGA was conducted on pure CSPs, Fe_3O_4-CSPs, and Pd/Fe_3O_4-CSPs nanocomposite as displayed in Fig. 4 to fully understand the thermal stability and events of the fabricated materials. It can be seen that the thermograph of CSPs indicates a slight mass loss of about 4% from 30 to 100 °C, probably due to the adsorbed water

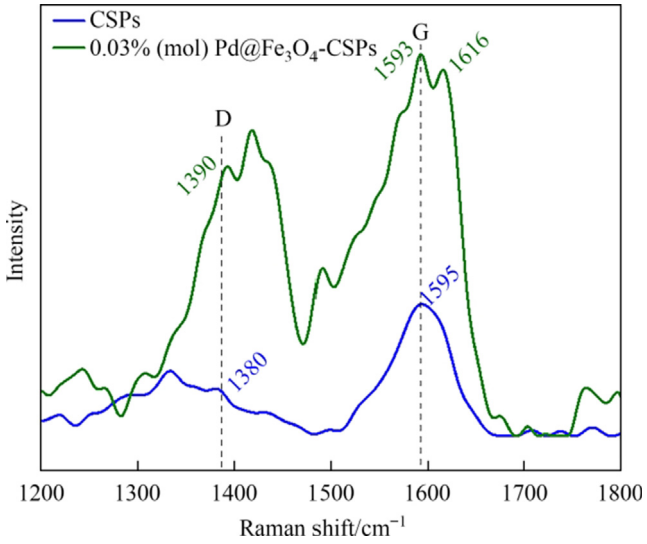

Fig. 3. Raman spectra of Fe_3O_4-CSPs and Fe_3O_4-CSPs catalyst containing 3% dosage of Pd.

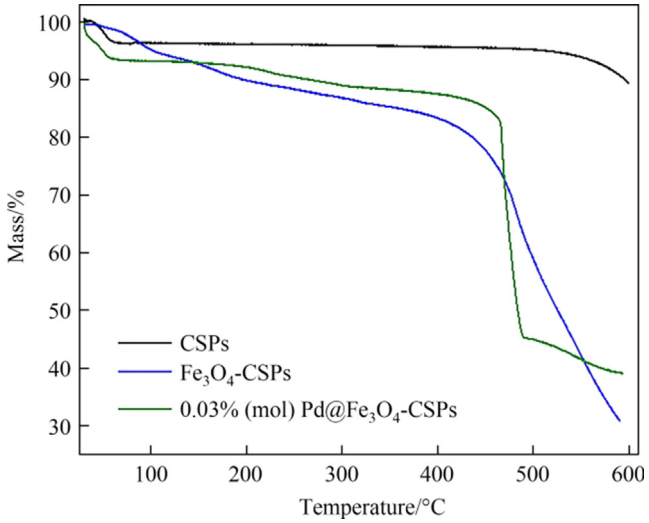

Fig. 4. TGA profiles of CSPs, Fe_3O_4-CSPs, and 0.03% (mol) Pd@Fe_3O_4-CSPs catalysts.

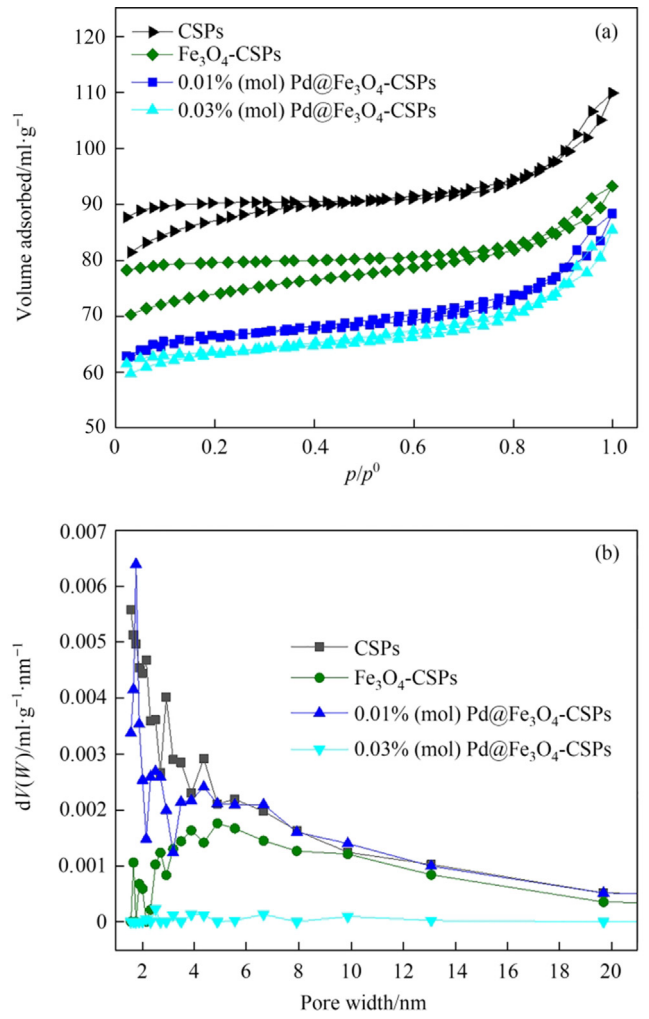

Fig. 5. (a) N_2 adsorption–desorption isotherms at 77 K (b) pore size distribution of CSPs and Fe_3O_4-CSPs catalyst containing various dosage of Pd.

removal. TG curve of the graphitic CSPs attains a plateau up to 500 °C with no remarkable mass loss, after which they would start to lose mass eventually. In Fe_3O_4-CSPs, and Pd/Fe_3O_4-CSPs nanocomposite, the TGA profiles displayed similar profiles with distinctive mass loss stages with increasing temperature. The first mass loss at about 100 °C can be ascribed to the elimination of the physi-sorbed water. The second significant mass loss at around 200 °C is related to the labile oxygen functional moieties decomposition.

Table 1
Texture characteristics for pure CSPs and Fe_3O_4-CSPs nanocomposite containing various contents of Pd nanoparticles

Catalysts	BET/$m^2 \cdot g^{-1}$	$V_p/cm^3 \cdot g^{-1}$	r/nm
CSPs	289.1	0.1651	1.72
Fe_3O_4-CSPs	267.3	0.1553	1.81
0.01% (mol) Pd/Fe_3O_4-CSPs	255.4	0.1456	1.91
0.03% (mol) Pd/Fe_3O_4-CSPs	253.2	0.1402	1.93

3.3. Surface and morphological assessment

For CSPs, Fe_3O_4-CSPs, and Pd/Fe_3O_4-CSPs nanocomposite containing various Pd nanoparticles (0.01% and 0.03%, mol), the N_2 adsorption–desorption isotherms at 77 K are seen in (Fig. 5(a)). Based on IUPAC classification, all samples displayed type I isotherms which is a key feature of microporous materials. Coating the CSPs with Fe_3O_4 and Pd nanoparticles did not change the loops and the isotherm form, indicating that the microporous structure was preserved; however, the adsorption ability was decreased. The surface area of CSPs amounts to 289.1 $m^2 \cdot g^{-1}$. The surface area of Fe_3O_4-CSPs, 0.01% (mol) Pd/Fe_3O_4-CSPs, and 0.03% (mol) Pd/Fe_3O_4-CSPs were 267.3, 255.4, and 253.2, respectively, that were lower than CSPs due to the introduction of Fe_3O_4 and Pd nanoparticles species within the pores of CSPs that had almost a low surface area (Table 1). In addition, the beneficial porosity effect disappeared with the immobilization of Fe_3O_4 and Pd nanoparticles, resulting in a decline in the volume of the pore and pore

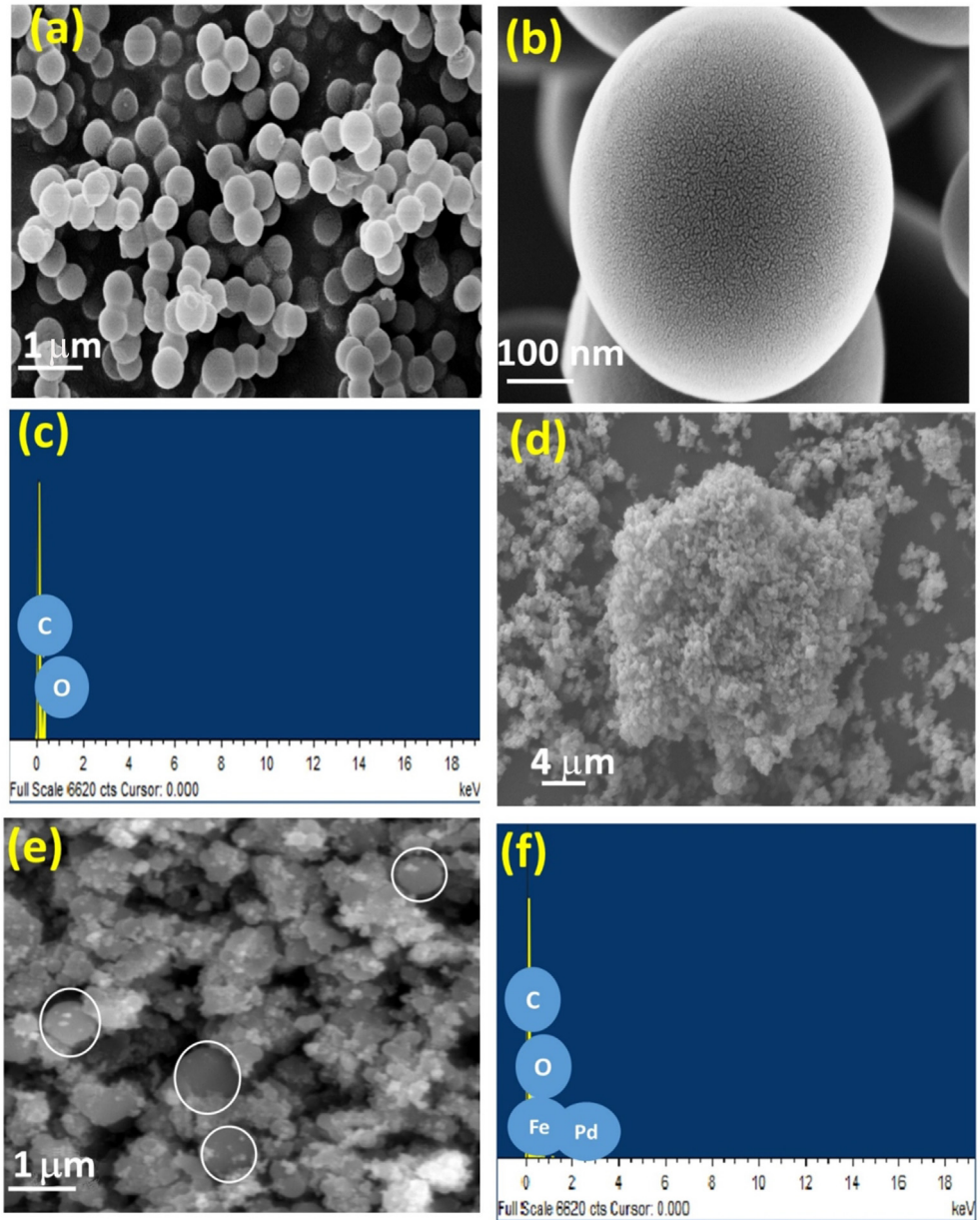

Fig. 6. FESEM-EDS of CSPs (a)–(c), and 0.03% (mol) Pd@Fe_3O_4-CSPs catalysts (d)–(f).

diameter (Table 1). Therefore, it is hypothesized that Fe_3O_4 and Pd species may allocate the shaped pore structure for the composite to the blockage effect. The pore size distribution (PSD) of all materials is displayed in Fig. 5(b). All samples have roughly the same PSD with different microporous area maximums. The accessibility of porosity for catalysis is required as it would offer greater accessible sites to improve the catalytic properties.

Field emission scanning electron microscopy (FESEM-EDS) was employed to morphologies CSPs (Fig. 6(a) and (b)). As can be shown, the CSPs with smooth surfaces are quite well dispersed and exhibit well-defined uniform spherical shapes. It is possible to verify CSPs porosity from the intensified FESEM images (Fig. 6 (b)). Furthermore, the morphology of the CSPs is remaining unaltered after coating with Fe_3O_4 and immobilization of Pd nanoparticles (Fig. 6(d) and (e)). The energy dispersive X-rays' investigation of the CSPs and 0.03% (mol). Pd@Fe_3O_4-CSPs was conducted, and the evaluated element's quantity percentage was shown in Fig. 6(c) and (f). It can be noted that the corresponding EDS results confirm the peaks ascribed to C, O, Fe, and Pd in the synthesized composite and no other elements are present.

In order to investigate the micro-structure, the fabricated CSPs have been further examined by the higher resolution TEM as illustrated in Fig. 7. HRTEM images confirm that the CSPs are successfully synthesized and exhibit a uniform spherical morphology with smooth surface and average size of 400 nm. The immobilization of CSPs with Fe_3O_4 and Pd nanoparticles has been recognized by HRTEM. As can be seen, the spherical morphology of the CSPs remained unchanged after coating with Fe_3O_4 and metallic Pd

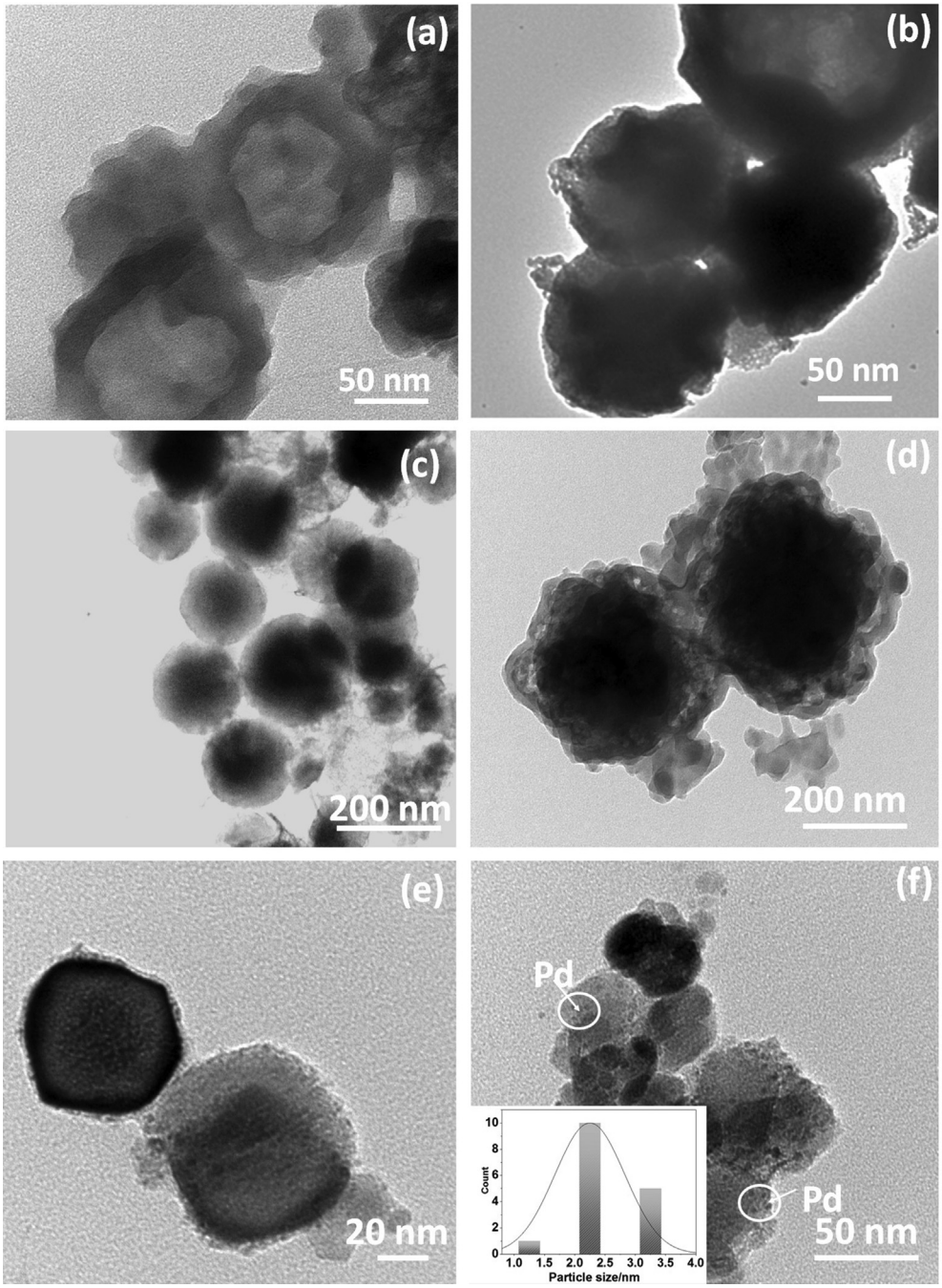

Fig. 7. HRTEM of CSPs (a)–(b), Fe_3O_4-CSPs (c)–(d), and 0.03% (mol) Pd@Fe_3O_4-CSPs (e)–(f) (inset the particle size distribution).

NPs. The morphology of the Fe_3O_4-CSPs composite displays a core–shell characteristic with fine particles coated on the CSPs surface, as displayed in Fig. 7(c) and (d). The diameter of the generated Fe_3O_4-CSPs with carbon shells is around 160 nm, while the thickness Fe_3O_4 layer in the shell is around 20 nm. Pd nanoparticles had a roughly spherical morphology with typical particle size distribution of 2–4 nm (inset in Fig. 7(f)) and were rather well dispersed over the surface of carbon spheres, as seen in Fig. 7(e) and (f).

3.4. Catalytic performance for Suzuki-Miyaura reaction

The catalytic efficiency of the magnetic Pd composite (with Pd contents of 1% and 3%, mass) has been examined using the Suzuki-Miyaura as a model reaction of phenylboronic acid (1.1 mol) and 4-bromoacetophenone (1.0 mmol) with a 5 mg catalyst in ethanol at 80 °C for 30 min as described in Fig. 8. A control test was conducted to have a better understanding about the function of palladium in catalytic performance. Under the same reaction conditions, the Suzuki-Miyaura coupling of phenylboronic acid and 4-bromoacetophenone in the existence of K_2CO_3 demonstrated that the reaction failed without the catalyst. Furthermore, commercially Pd/C catalyst, the most commonly exploited catalyst in coupling processes, only converts 10% under the same reaction conditions. This could be owing to the irregular size distributions of Pd nanoparticles, with considerable quantities of Pd NPs agglomerating on the carbon support's surface. The palladium concentration, the applicability of different substrate, and reusability of the prepared composite were examined.

3.4.1. Effect of palladium concentration

In the sense of heterogeneous catalysis of the Suzuki-Miyaura cross coupling process, Pd-NP loaded on a core–shell magnetic carbon sphere called Fe_3O_4-CSPs were seen to be potential catalysts for the coupling of aryl halides with phenylboronic acid. Fig. 9 shows the biphenyl yield as described in Fig. 8 for CSPs, Fe_3O_4-CSPs, and different loadings of the Fe_3O_4-CSPs with palladium nanoparticles under the reaction circumstances (1 mol 4-bromoacetophenone, 1.1 mol phenylboronic acid, 1 mmol K_2CO_3, 5 mg catalyst, for 30 min at 80 °C). The results revealed that both CSPs, and Fe_3O_4-CSPs demonstrated poor activity affording a yield of 1% and 7%, respectively, to the biphenyl product as tracked by 1HNMR spectroscopy. However, the fashioned composites containing palladium nanoparticles have demonstrated superior activity toward Suzuki coupling. With the smallest Pd loading 0.01% (mol), the process affording a yield of 95% biphenyl product. Similarly, when 3% (mass) loadings was employed, the catalyst still performed efficiently, offering a yield of 100% under the same reaction conditions. Metallic nanoparticles are extremely active because of their great surface-to-volume ratio [29]. On the other hand, as the nanoparticles size rising by aggregation, the abundance of active sites, found in most cases at surface defect centers like vertexes and edges, reduces. The very facile reduction to Pd(0) under catalytic conditions, not only during hydrogen reduction but also in Suzuki cross-coupling reactions, is a particular palladium feature. Consequently, Pd(II) used *in situ* forms Pd(0) as a catalyst precursor, which is turned to Pd NPs under the preparation conditions.

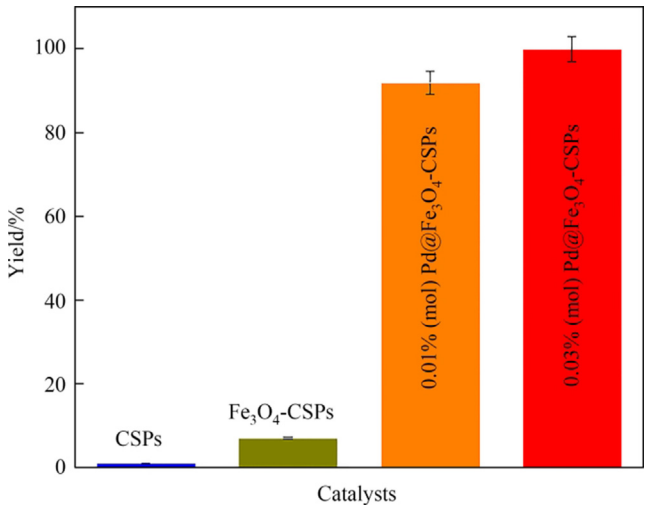

Fig. 9. Suzuki cross-coupling reaction of 4-bromoacetophenone with phenylboronic acid catalyzed by CSPs, Fe_3O_4-CSPs, and Pd/Fe_3O_4-CSPs composite containing various dosage of Pd nanoparticles.

3.4.2. Nature of active sites of Suzuki cross coupling reaction and mechanism

To obtain more understanding about the oxidation state and the binding energy of Pd loaded on Fe_3O_4-CSPs surface, the XPS analysis were performed. The O 1s, C 1s, and Fe 2p, regions were noted

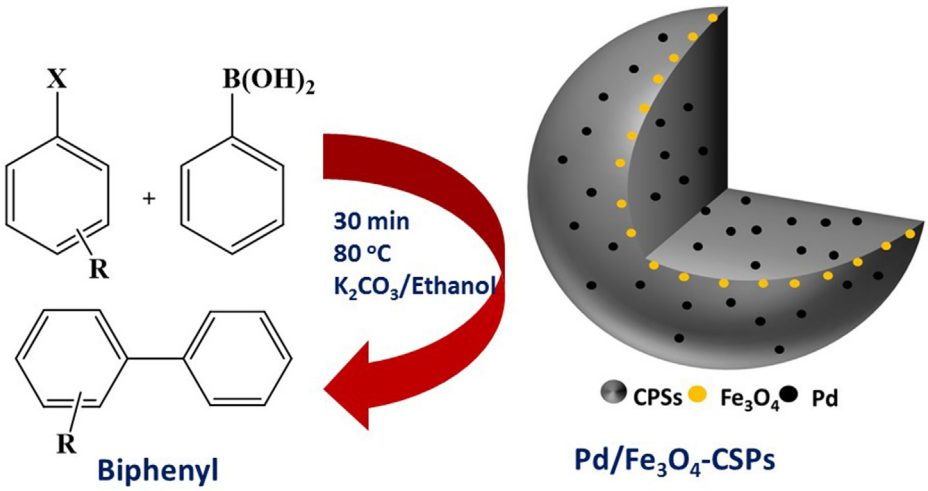

Fig. 8. Suzuki cross-coupling reaction over Pd@Fe_3O_4-CSPs catalyst.

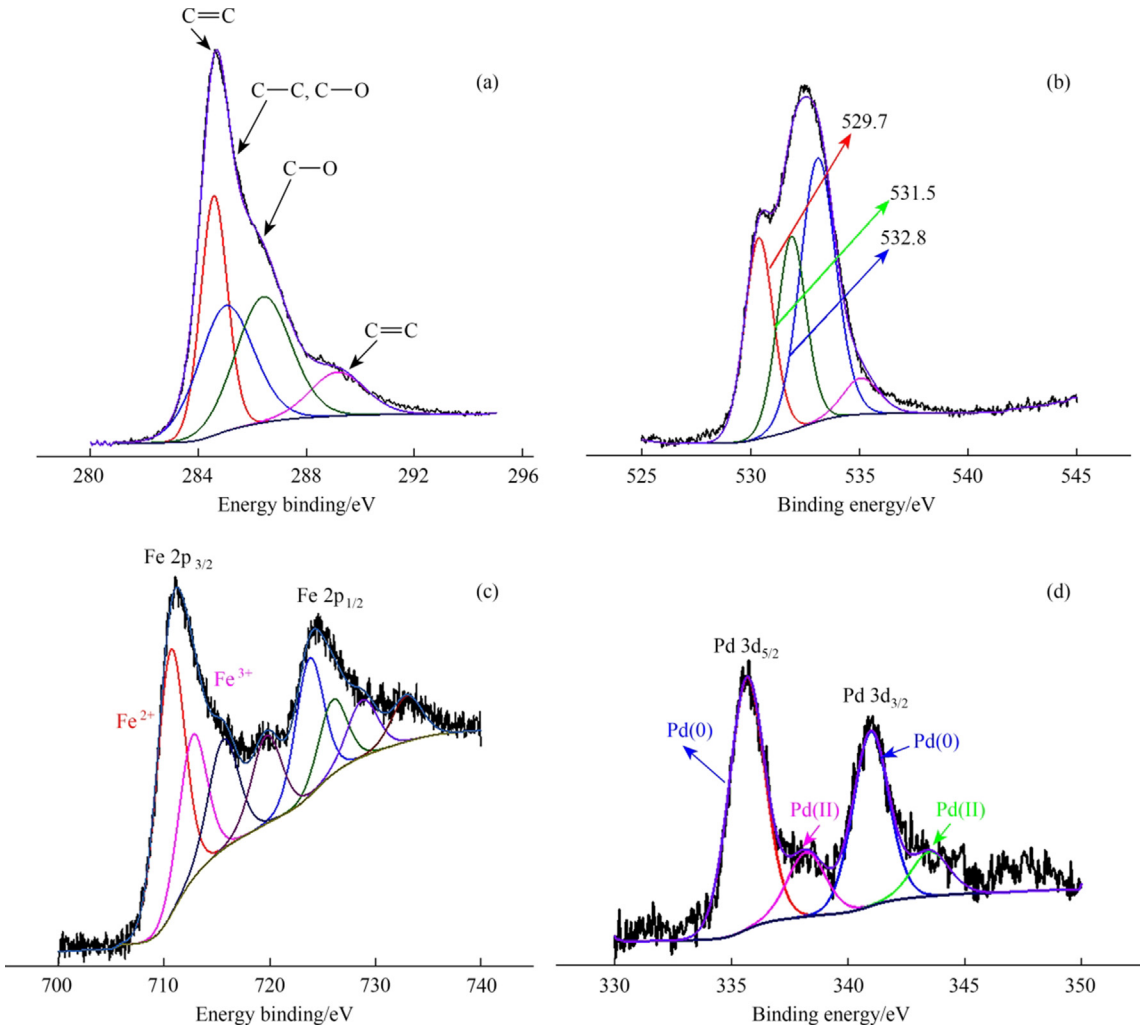

Fig. 10. XPS spectra of Pd/Fe_3O_4-CSPs fashioned composite: C 1s (a), O 1s (b), Fe 2p (c) and Pd 3d (d).

and examined using the Gaussian-Lorentzian approach, as displayed in Fig. 10(a)–(c). The Pd element's oxidation status in the Fe_3O_4-CSPs nanocomposite was also verified. The binding energies for Pd(0) $3d_{3/2}$ and $3d_{5/2}$, respectively, were 341.01 and 335.68 eV in Fig. 10(d), confirming the presence of metallic Pd NPs in Fe_3O_4-CSPs nanocomposite. Furthermore, for Pd(II), the binding energy values were 343.83 and 338.1 eV, respectively. The XPS findings display that the catalyst is made up of a combination of Pd(0) and Pd(II) in varying concentrations on the surface of Fe_3O_4-CSPs. Pd(0) has a surface concentration of 78.6%, while Pd(II) has a surface concentration of 21.4% for Pd(II). The appearance of Pd(II) ions on the composite surface might be owing to Pd(II) being attached to surface oxygen moieties provided by the CSPs surface, or being coated by the metallic Pd NPs, so the Pd(II) still has not been reduced to Pd(0). It seems that the exceptional activity of the fabricated Pd/Fe_3O_4-CSPs core–shell catalyst is specifically ascribed to the large amount of Pd(0) and Pd(II) active sites existing in the as-synthesized composite as well as the great dispersion of the metallic species over CSPs. A common catalytic mechanism for the cross-coupling (Fig. 11) comprises the oxidative- addition of aryl halides to the Pd(0) species to generate Ar^1-Pd(II)-X, and seems to be the rate-determining step in the catalytic mechanism. This step is followed by trans-metalation with primary-group arylmetallics (Ar^2M) to offer the diarylpalladium (Ar^1-Pd(II)-Ar^2) complex that can endure a reductive-elimination, resulted in Ar^1-Ar^2 (C—C) bond development and catalyst regeneration [45].

3.4.3. The scope for Suzuki cross coupling reaction

A wider spectrum of substituted aryl halides has been coupled with phenylboronic acid under the optimal reaction conditions to emphasize the scope for this C—C coupling reaction. The findings are presented in Table 2. All Pd/Fe_3O_4-CSPs core–shell catalysts were noticed to have shown superior catalytic performance. The 0.03% (mol) Pd/Fe_3O_4-CSPs core–shell seemed to be the strongest among the screened catalysts and was thus selected as the catalyst in the further Suzuki-Miyaura reaction experiment. The data displayed in Table 2 indicate that the 0.03% (mol) Pd/Fe_3O_4-CSPs core–shell catalyst was extremely effective corresponding to TOF of 0.1490 h^{-1} and TON of 745 in case of using 1-bromobenzene and TOF of 13221 h^{-1} and TON of 661 in case of using 1-bromoanthracene, and the majority of these reactions were rapid and completed within 30 min. Obviously, aryl bromide bearing either electron-withdrawing or electron-donating moieties exhibited comparable reactivity and reacted efficiently to the corresponding yield.

3.4.4. Catalyst reusability and palladium leaching

All of the coupling reactions performed facilely to deliver the anticipated product with high yields. But for practical implementations of heterogeneous processes, the durability of the catalyst and its reusability degree are essential considerations. Eventually, we explored the reusability of the 0.03% (mol) Pd/Fe_3O_4-CSPs core–shell catalyst for the reaction of 4-bromoacetophenone with

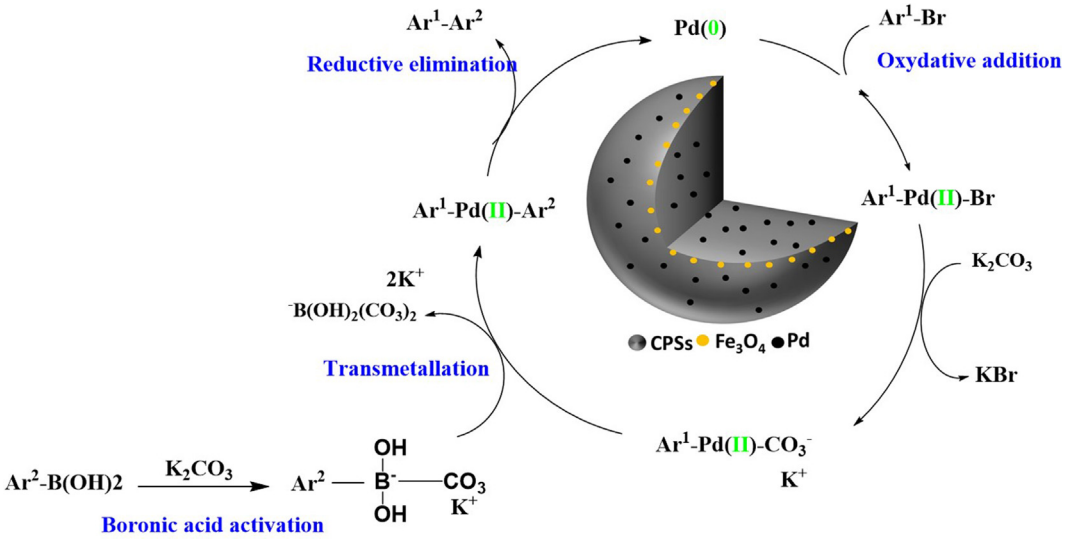

Fig. 11. Catalytic reaction mechanism of the Suzuki cross-coupling reaction over Pd@Fe_3O_4-CSPs catalyst.

Table 2
Substrates scope of aryl halides for the Suzuki-Miyaura cross-coupling reaction catalyzed by 0.03% (mol) Pd/Fe_3O_4-CSPs

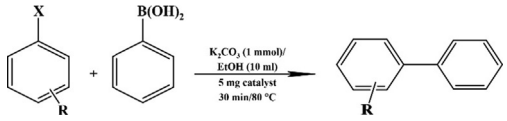

Entry				Yield/%	TOF	TON
1	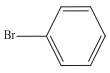	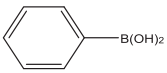	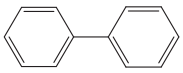	98	1490	745
2	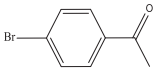	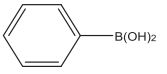	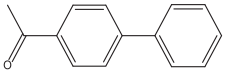	99	1505	753
3	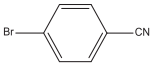	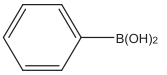	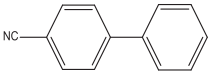	99	1505	753
4	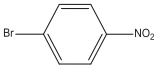	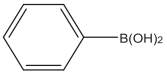	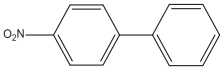	99	1505	753
5	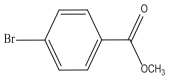	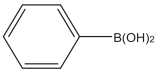	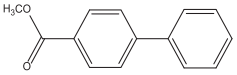	98	1490	745
6	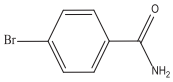	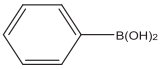	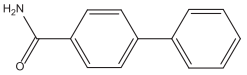	99	1505	753
7	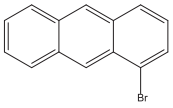	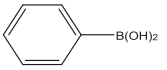	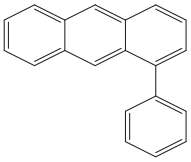	87	1322	661

phenylboronic acid as the model reaction for 30 min at 80 °C. The catalyst was collected by a magnet and dried in a vacuum after the first cycle. The catalyst was then directly recycled for up to four consecutive runs of the reaction under similar conditions as described above. The findings are presented in Table 3. The results revealed that up to four runs, the recovered catalyst have not substantially lost its performance. Using the AAS analysis, metallic palladium leaching from the catalyst was further investigated. The findings indicate that just a trace quantity of the metallic Pd is leached out from the Fe_3O_4-CSPs. The function moieties on CSPs offer efficient binding centers combined with palladium, thus allowing facile catalyst recycling and mitigating metal leaching.

We compared our results to those cited in the literature for magnetically recyclable Pd-based catalysts [46–53]. Table 4 shows the findings of bromobenzene interacting with phenylboronic as a model test reaction. It can be shown that the results acquired in

Table 3
Reusability of the 0.03% (mol) Pd/Fe_3O_4-CSPs catalyst for the Suzuki-Miyaura cross-Coupling

Entry	Cycle	Time/min	Temperature/°C	Yield/%
1	first	30	80	100
2	second	30	80	100
3	third	30	80	99
4	fourth	30	80	98

Reaction conditions: 4-bromoacetophenone (1.0 mmol), phenylboronic acid (1.1 mmol), K_2CO_3 (1.0 mmol), EtOH (10 ml), and 5 mg catalyst at reflux under air for 30 min at 80 °C.

Table 4
Catalytic activity of various Pd-based catalysts in the Suzuki-Miyaura cross-coupling of bromobenzene and phenylboronic acid

Catalyst	Solvent	Base	Time/h	Temperature/°C	Yield/%	Ref.
Co@C@Pd	THF-H_2O	Na_2CO_3	12	65	92	[46]
Pd-Fe_3O_4	BME-H_2O	Na_2CO_3	24	Reflux	70	[47]
Pd/PRGO	EtOH-H_2O	K_2CO_3	4	Microwave	100	[48]
Pd@SBA-15	H_2O	K_2CO_3	1	80	98	[49]
Pd@CNPCs	DMF-H_2O	K_2CO_3	3	50	98.2	[50]
MUA-Pd	DMF	NaOH	12	90	92	[51]
Pd-TMV	CH_3CN-H_2O	Na_2CO_3	24	50	53	[52]
Pd-MTAMT	DMF-H	NaOH	10	85	85	[53]
Pd/Fe_3O_4-CSPs	EtOH	K_2CO_3	0.5	80	98	This Work

this investigation were more active than those previously published. Some harmful solvents such as CH_3CN and *p*-xylene were utilized, despite the fact that some of them can also provide high yields. These compounds are not as beneficial as the ethyl alcohol applied in this study. The use of our Pd/Fe_3O_4-CSPs nanoparticles is simple due to the advantages of easy separation, high stability, and ease of manufacture. Furthermore, in certain studies, Pd complexes were utilized, and the synthesis procedure of the complexes damaged several groups, potentially lowering the catalytic activity.

4. Conclusions

In conclusion, a facile eco-friendly approach were successfully employed to fabricate the Fe_3O_4-CSPs core–shell decorated with Pd nanoparticles. Utilizing this approach, an unparalleled Fe_3O_4-CSPs immobilized nano palladium has been exploited for the Suzuki-Miyaura cross-coupling reactions. The core–shell composite thus synthesized has been displayed to be powerful in the C—C bond formation processes. The substrate variety demonstrated the strong tolerance of the core–shell composite to different functional moieties. Furthermore, without a substantial decrease of performance, we could repetitive reuse of the catalyst up to four catalytic cycles. Such reasonable tailoring on the nanocatalysts of the metallic NPs and CSPs will tailor and develop of high-performance multi-functional nanocatalysts.

Declaration of Competing Interest

The authors declare that they have no known competing financial interests or personal relationships that could have appeared to influence the work reported in this paper.

Acknowledgements

The authors would like to thank the Deanship of graduate studies at Jouf University for funding and supporting this research through the initiative of DGS, Graduate Students Research Support (GSR) at Jouf University, Saudi Arabia. Additionally, the authors acknowledge the facilities operated by the central laboratory at Jouf University.

Appendix A. Supplementary data

Supplementary data to this article can be found online at https://doi.org/10.1016/j.cjche.2021.11.024.

References

[1] A.F. Hassan, H. Elhadidy, Effect of Zr+4 doping on characteristics and sonocatalytic activity of TiO_2/carbon nanotubes composite catalyst for degradation of chlorpyrifos, *J. Phys. Chem. Solids* 129 (2019) 180–187.
[2] S. Sajjadi, A. Khataee, R. Darvishi Cheshmeh Soltani, A. Hasanzadeh, N, S co-doped graphene quantum dot-decorated Fe_3O_4 nanostructures: Preparation, characterization and catalytic activity, *J. Phys. Chem. Solids* 127 (2019) 140–150.
[3] C.Q. Lin, W. Wei, Y.H. Hu, Catalytic behavior of graphene oxide for cement hydration process, *J. Phys. Chem. Solids* 89 (2016) 128–133.
[4] K.J. Chen, W.J. Fan, C.J. Huang, X.Q. Qiu, Enhanced stability and catalytic activity of bismuth nanoparticles by modified with porous silica, *J. Phys. Chem. Solids* 110 (2017) 9–14.
[5] P. Avouris, C. Dimitrakopoulos, Graphene: Synthesis and applications, *Mater. Today* 15 (3) (2012) 86–97.
[6] D.C. Marcano, D.V. Kosynkin, J.M. Berlin, A. Sinitskii, Z.Z. Sun, A.S. Slesarev, L.B. Alemany, W. Lu, J.M. Tour, Correction to improved synthesis of graphene oxide, *ACS Nano* 12 (2) (2018) 2078.
[7] H.W. Zhu, C.L. Xu, D.H. Wu, B.Q. Wei, R. Vajtai, P.M. Ajayan, Direct synthesis of long single-walled carbon nanotube strands, *Science* 296 (5569) (2002) 884–886.
[8] H.C. Kuan, C.C.M. Ma, W.P. Chang, S.M. Yuen, H.H. Wu, T.M. Lee, Synthesis, thermal, mechanical and rheological properties of multiwall carbon nanotube/waterborne polyurethane nanocomposite, *Compos. Sci. Technol.* 65 (11–12) (2005) 1703–1710.
[9] R. Wang, K.Q. Lu, Z.R. Tang, Y.J. Xu, Recent progress in carbon quantum dots: Synthesis, properties and applications in photocatalysis, *J. Mater. Chem. A* 5 (8) (2017) 3717–3734.
[10] Y.G. Ko, U.S. Choi, J.S. Kim, Y.S. Park, Novel synthesis and characterization of activated carbon fiber and dye adsorption modeling, *Carbon* 40 (14) (2002) 2661–2672.
[11] M. Terrones, A.R. Botello-Méndez, J. Campos-Delgado, F. López-Urías, Y.I. Vega-Cantú, F.J. Rodríguez-Macías, A.L. Elías, E. Muñoz-Sandoval, A.G. Cano-Márquez, J.C. Charlier, H. Terrones, Graphene and graphite nanoribbons: Morphology, properties, synthesis, defects and applications, *Nano Today* 5 (4) (2010) 351–372.
[12] C.D. Liang, Z.J. Li, S. Dai, Mesoporous carbon materials: Synthesis and modification, *Angew. Chem. Int. Ed. Engl.* 47 (20) (2008) 3696–3717.
[13] F. Wudl, Fullerene materials, *J. Mater. Chem.* 12 (7) (2002) 1959–1963.
[14] Y. Li, J. Qi, J. Li, J. Shen, Y. Liu, X. Sun, J. Shen, W. Han, L. Wang, Nitrogen-doped hollow mesoporous carbon spheres for efficient water desalination by capacitive deionization, *ACS Sustain. Chem. Eng.* 5 (2017) 6635–6644.
[15] J. Liu, N.P. Wickramaratne, S.Z. Qiao, M. Jaroniec, Molecular-based design and emerging applications of nanoporous carbon spheres, *Nat. Mater.* 14 (8) (2015) 763–774.

[16] L.M. Guo, X.Z. Cui, Y.S. Li, Q.J. He, L.X. Zhang, W.B. Bu, J.L. Shi, Hollow mesoporous carbon spheres with magnetic cores and their performance as separable bilirubin adsorbents, *Chem. Asian J.* 4 (9) (2009) 1480–1485.
[17] L.M. Guo, L.X. Zhang, J.M. Zhang, J. Zhou, Q.J. He, S.Z. Zeng, X.Z. Cui, J.L. Shi, Hollow mesoporous carbon spheres: An excellent bilirubin adsorbent, *Chem. Commun. (Camb)* 40 (2009) 6071–6073.
[18] F.P. Hu, Z.Y. Wang, Y.L. Li, C.M. Li, X. Zhang, P.K. Shen, Improved performance of Pd electrocatalyst supported on ultrahigh surface area hollow carbon spheres for direct alcohol fuel cells, *J. Power Sources* 177 (1) (2008) 61–66.
[19] S.B. Yang, X.L. Feng, L.J. Zhi, Q. Cao, J. Maier, K. Müllen, Nanographene-constructed hollow carbon spheres and their favorable electroactivity with respect to lithium storage, *Adv Mater* 22 (7) (2010) 838–842.
[20] J.P. Han, G.Y. Xu, B. Ding, J. Pan, H. Dou, D.R. MacFarlane, Porous nitrogen-doped hollow carbon spheres derived from polyaniline for high performance supercapacitors, *J. Mater. Chem. A* 2 (15) (2014) 5352–5357.
[21] X.H. Liu, L. Zhou, Y.Q. Zhao, L. Bian, X.T. Feng, Q.S. Pu, Hollow, spherical nitrogen-rich porous carbon shells obtained from a porous organic framework for the supercapacitor, *ACS Appl. Mater. Interfaces* 5 (20) (2013) 10280–10287.
[22] S.L. Buchwald, Cross coupling, *Acc. Chem. Res.* 41 (11) (2008) 1439.
[23] L.X. Yin, J. Liebscher, Carbon-carbon coupling reactions catalyzed by heterogeneous palladium catalysts, *Chem. Rev.* 107 (1) (2007) 133–173.
[24] R.F. Heck, Palladium-catalyzed reactions of organic halides with olefins, *Acc. Chem. Res.* 12 (1979) 146–151.
[25] N. Miyaura, A. Suzuki, Palladium-catalyzed cross-coupling reactions of organoboron compounds, *Chem. Rev.* 95 (7) (1995) 2457–2483.
[26] I.P. Beletskaya, A.V. Cheprakov, The heck reaction as a sharpening stone of palladium catalysis, *Chem. Rev.* 100 (8) (2000) 3009–3066.
[27] C.J. Welch, J. Albaneze-Walker, W.R. Leonard, M. Biba, J. DaSilva, D. Henderson, B. Laing, D.J. Mathre, S. Spencer, X.D. Bu, T.B. Wang, Adsorbent screening for metal impurity removal in pharmaceutical process research, *Org. Process. Res. Dev.* 9 (2) (2005) 198–205.
[28] C. Garrett, K. Prasad, The art of meeting palladium specifications in active pharmaceutical ingredients produced by Pd-catalyzed reactions, *Adv. Synth. Catal.* 346 (8) (2004) 889–900.
[29] R. Narayanan, M.A. El-Sayed, Effect of catalysis on the stability of metallic nanoparticles: Suzuki reaction catalyzed by PVP-palladium nanoparticles, *J. Am. Chem. Soc.* 125 (27) (2003) 8340–8347.
[30] R. Narayanan, M.A. El-Sayed, Effect of colloidal catalysis on the nanoparticle size distribution: Dendrimer-Pd *vs* PVP-Pd nanoparticles catalyzing the suzuki coupling reaction, *J. Phys. Chem. B* 108 (25) (2004) 8572–8580.
[31] C.S. Duanmu, I. Saha, Y. Zheng, B.M. Goodson, Y. Gao, Dendron-functionalized superparamagnetic nanoparticles with switchable solubility in organic and aqueous media: Matrices for homogeneous catalysis and potential MRI contrast agents, *Chem. Mater.* 18 (25) (2006) 5973–5981.
[32] R. Narayanan, C. Tabor, M.A. El-Sayed, Can the observed changes in the size or shape of a colloidal nanocatalyst reveal the nanocatalysis mechanism type: Homogeneous or heterogeneous?, *Top Catal.* 48 (1–4) (2008) 60–74.
[33] P.J. Ellis, I.J. Fairlamb, S.F. Hackett, K. Wilson, A.F. Lee, Evidence for the surface-catalyzed Suzuki-Miyaura reaction over palladium nanoparticles: An operando XAS study, *Angew. Chem. Int. Ed. Engl.* 49 (10) (2010) 1820–1824.
[34] B.M. Bhanage, M. Arai, Catalyst product separation techniques in heck reaction, *Catal. Rev.* 43 (3) (2001) 315–344.
[35] L. Djakovitch, K. Koehler, Heck reaction catalyzed by Pd-modified zeolites, *J. Am. Chem. Soc.* 123 (25) (2001) 5990–5999.
[36] L. Djakovitch, K. Koehler, Heterogeneously catalysed Heck reaction using palladium modified zeolites, *J. Mol. Catal. A: Chem.* 142 (2) (1999) 275–284.
[37] M.K. Bhunia, S.K. Das, P. Pachfule, R. Banerjee, A. Bhaumik, Nitrogen-rich porous covalent imine network (CIN) material as an efficient catalytic support for C-C coupling reactions, *Dalton Trans.* 41 (4) (2012) 1304–1311.
[38] C.A. Wang, Y.F. Han, Y.W. Li, K. Nie, X.L. Cheng, J.P. Zhang, Bipyridyl palladium embedded porous organic polymer as highly efficient and reusable heterogeneous catalyst for Suzuki-Miyaura coupling reaction, *RSC Adv.* 6 (41) (2016) 34866–34871.
[39] S.Y. Ding, J. Gao, Q. Wang, Y. Zhang, W.G. Song, C.Y. Su, W. Wang, Construction of covalent organic framework for catalysis: Pd/COF-LZU1 in suzuki–miyaura coupling reaction, *J. Am. Chem. Soc.* 133 (49) (2011) 19816–19822.
[40] S.K. Mohamed, M. Abuelhamd, N.K. Allam, A. Shahat, M. Ramadan, H.M.A. Hassan, Eco-friendly facile synthesis of glucose-derived microporous carbon spheres electrodes with enhanced performance for water capacitive deionization, *Desalination* 477 (2020) 114278.
[41] X. Sun, Y. Li, Colloidal carbon spheres and their core/shell structures with noble-metal nanoparticles, *Angew. Chem. Int. Ed. Engl.* 43 (5) (2004) 597–601.
[42] M. Sevilla, A. Fuertes, Chemical and structural properties of carbonaceous products obtained by hydrothermal carbonization of saccharides, *Chem. Eur. J.* 15 (16) (2009) 4195–4203.
[43] M. Li, W. Li, S.X. Liu, Hydrothermal synthesis, characterization, and KOH activation of carbon spheres from glucose, *Carbohydr. Res.* 346 (8) (2011) 999–1004.
[44] D. Graf, F. Molitor, K. Ensslin, C. Stampfer, A. Jungen, C. Hierold, L. Wirtz, Spatially resolved Raman spectroscopy of single- and few-layer graphene, *Nano Lett.* 7 (2) (2007) 238–242.
[45] S. Kotha, K. Lahiri, D. Kashinath, Recent applications of the Suzuki-Miyaura cross-coupling reaction in organic synthesis, *Tetrahedron* 58 (48) (2002) 9633–9695.
[46] A. Schätz, T.R. Long, R.N. Grass, W.J. Stark, P.R. Hanson, O. Reiser, Immobilization on a nanomagnetic Co/C surface using ROM polymerization: Generation of a hybrid material as support for a recyclable palladium catalyst, *Adv. Funct. Mater.* 20 (24) (2010) 4323–4328.
[47] Y. Jang, J. Chung, S. Kim, S.W. Jun, B.H. Kim, D.W. Lee, B.M. Kim, T. Hyeon, Simple synthesis of Pd-Fe_3O_4 heterodimer nanocrystals and their application as a magnetically recyclable catalyst for Suzuki cross-coupling reactions, *Phys. Chem. Chem. Phys.* 13 (7) (2011) 2512–2516.
[48] S. Moussa, A.R. Siamaki, B.F. Gupton, M.S. El-Shall, Pd-partially reduced graphene oxide catalysts (Pd/PRGO): Laser synthesis of Pd nanoparticles supported on PRGO nanosheets for carbon–carbon cross coupling reactions, *ACS Catal.* 2 (1) (2012) 145–154.
[49] J. Zhi, D.P. Song, Z.W. Li, X. Lei, A.G. Hu, Palladium nanoparticles in carbon thin film-lined SBA-15 nanoreactors: Efficient heterogeneous catalysts for Suzuki-Miyaura cross coupling reaction in aqueous media, *Chem. Commun. Camb. Engl.* 47 (38) (2011) 10707–10709.
[50] R. Li, P. Zhang, Y.M. Huang, P. Zhang, H. Zhong, Q.W. Chen, Pd–Fe_3O_4@C hybrid nanoparticles: Preparation, characterization, and their high catalytic activity toward Suzuki coupling reactions, *J. Mater. Chem.* 22 (42) (2012) 22750.
[51] M. Cargnello, N.L. Wieder, P. Canton, T. Montini, G. Giambastiani, A. Benedetti, R.J. Gorte, P. Fornasiero, A versatile approach to the synthesis of functionalized thiol-protected palladium nanoparticles, *Chem. Mater.* 23 (17) (2011) 3961–3969.
[52] C.X. Yang, A.K. Manocchi, B. Lee, H. Yi, Viral-templated palladium nanocatalysts for Suzuki coupling reaction, *J. Mater. Chem.* 21 (1) (2011) 187–194.
[53] A. Modak, J. Mondal, M. Sasidharan, A. Bhaumik, Triazine functionalized ordered mesoporous polymer: A novel solid support for Pd-mediated C—C cross-coupling reactions in water, *Green Chem.* 13 (5) (2011) 1317.